# Peer-Reviewed Technical Communication

## Feasibility Study of Underwater Acoustic Communications Between Buried and Bottom-Mounted Sensor Network Nodes

Alenka G. Zajić, *Member, IEEE*, and Geoffrey F. Edelmann

***Abstract*—This paper presents a feasibility study of underwater communications between buried sensor network nodes. To investigate this problem, two experiments have been conducted: where some sensor nodes are buried in the sediment, and where all sensor nodes are buried in the sediment. The orthogonal frequency-division multiplexing (OFDM) communications have been chosen to test underwater communications because of its unique strength in handling transmissions over long dispersive channels. Since the existing OFDM schemes for underwater communications are designed to achieve high data rate communications within the water column and are not adequate for communications between sensors placed on the ocean floor, a new low-complexity OFDM receiver has been proposed. The proposed receiver performs frame-by-frame channel estimation, residual phase tracking, diversity combining, and data demodulation. This approach is adopted because of its effectiveness in applications with very fast varying channels and a large number of propagation paths. It is demonstrated that the error-free performance can be achieved between buried sensors using the proposed OFDM receiver.**

***Index Terms*—Distributed sensor networks, orthogonal frequency-division multiplexing (OFDM), underwater acoustic communications.**

### I. Introduction

THERE has been a growing interest in designing distributed underwater wireless sensor networks because of their ability to bring computation and sensing into the physical world. Underwater sensor networks have many potential applications, including seismic monitoring, scientific exploration of the ocean, tactical surveillance, pollution monitoring, offshore exploration, and support for underwater robots. For example, underwater sensor networks can provide significant benefits in seismic imaging of undersea oil fields. Today, most seismic imaging tasks for offshore oil fields are carried out by a ship that tows a large array of hydrophones on the surface [1]. The cost of such technology is very high, and the seismic survey can only be carried out rarely, for example, once every two to three years. In comparison, sensor network nodes have very low cost, and can be permanently deployed on the ocean floor, which allows frequent seismic imaging (e.g., once every three months) [2]. Additionally, networks near the bottom are more trawl resistant and covert.

However, achieving reliable underwater acoustic communications between sensors deployed on the ocean floor is not an easy task. First, the underwater acoustic (UWA) channel is one of the most challenging communication channels. It suffers large delay spread, leading to strong frequency selectivity and exhibits high temporal and spatial variations. Being both frequency and time selective, UWA channel poses great challenges for high performance and reliable underwater communications. Furthermore, the underwater communications near the ocean floor are even more challenging due to lower signal strength. Finally, near-bottom sensor network nodes may get buried or partially buried (due to movements in the ocean), which introduces additional attenuation in the system and may prevent communication between nodes.

To investigate the feasibility of UWA communications between buried or bottom-mounted sensor network nodes, we have conducted two experiments: the Naval Research Laboratory (NRL) Acoustic Communications Measurement System (ACOMMS09) experiment and the NRL sediment experiment (SedEx09). During the ACOMMS09 experiment, a portion of the sensors (i.e., hydrophones) were buried in the soft sediment (i.e., mud). The experiment was held near the New Jersey shore in May 2009. On the other hand, during the SedEx09 experiment, the hydrophones were buried in the hard sediment (i.e., sand). This experiment was held near Panama City, FL, in August 2009. All signals analyzed in this paper were transmitted at 17 kHz. Due to its unique strength in handling transmissions over long dispersive channels, we have chosen orthogonal frequency-division multiplexing (OFDM) communications to test UWA communications between buried network nodes.

Recently, there has been an increased interest in underwater OFDM communications, e.g., the low-complexity adaptive OFDM receiver in [3], the pilot-tone-based block-by-block OFDM receivers in [4]–[7], and the noncoherent OFDM receiver based on ON–OFF keying in [8]. However, all these OFDM schemes are designed to achieve high data rate communications in the water column and may not be suited for communications between network nodes placed on the ocean floor.

To address this issue, we have designed a new low-complexity OFDM system. At the transmitter side, each packet is

Manuscript received August 16, 2010; revised May 14, 2012; accepted August 07, 2012. Date of publication September 27, 2012; date of current version January 09, 2013. This work was supported by the U.S. Office of Naval Research.

**Associate Editor: W. M. Carey**.

A. G. Zajić is with the School of Computer Science, Georgia Institute of Technology, Atlanta, GA 30332-0280 USA (e-mail: azajic@cc.gatech.edu).

G. F. Edelmann is with the U.S. Naval Research Laboratory, Washington, DC 20375 USA (e-mail: edelmann@nrl.navy.mil).

Digital Object Identifier 10.1109/JOE.2012.2212832

partitioned into frames that consist of several OFDM blocks. The training sequence at the beginning of each frame is used for channel estimation. Furthermore, the cyclic guard interval is used to separate OFDM blocks, while the pilot tones are used for the residual phase tracking. Finally, the convolutional coding is applied to improve the reliability of communications. At the receiver side, we focus on a frame-by-frame processing similar to other methods [4], [5]. This approach is very effective for applications with very fast varying channels (often experienced at the bottom of the ocean) because it does not rely on channel dependence across the frames. Using the training sequence and pilot tones, we perform the channel estimation and residual phase tracking, followed by diversity processing, demodulation, and decoding.

The proposed single-input–single-output (SISO) OFDM system was tested during the ACOMMS09 and SedEx09 experiments. The results show that the main obstacle in achieving reliable communication with sensor nodes buried in the soft sediment lies in providing sufficient signal-to-noise-ratio (SNR) to the receiving system. If sufficient SNR is available (i.e., $>$10 dB), the uncoded and coded bit error rate (BER) for SISO quaternary phase-shift keying (QPSK) signals are about $10^{-2}$ and $10^{-4}$, respectively, regardless of how close to the ocean floor sensor nodes are placed. Intriguingly, use of a sensor mast provided only some limited SNR improvement indicating that a node immediately above the sediment will perform about as well as one 2 m above the sediment.

Finally, we showed that the performance of the proposed SISO OFDM system can be improved by superimposing signals received at the receive hydrophone array. The SNR and BER results for uncoded and coded QPSK signals received using the first four elements of two different hydrophone arrays placed in the water column and using the four elements placed near the soft and hard sediments are presented. The results show that the average combined input SNR in all experimental setups is higher than 10 dB and that all four setups have uncoded BER about $10^{-3}$, while coded signals are received without errors. All presented results show that to achieve underwater communications between buried sensor nodes, we need to design a system that has high SNR, can successfully handle large number of propagation paths, and uses multiple hydrophones as the receiving elements.

The remainder of this paper is organized as follows. Section II describes the transmitter, receiver, and signal design for the proposed OFDM system. This section also details the channel estimation, residual phase tracking, and diversity combining algorithms used in the proposed OFDM system. Section III describes the experimental setup used for the ACOMM09 and SedEx09 experiments. Section IV presents the SNR and BER results for several experimental settings used in the ACOMM09 and SedEx09 experiments. Section V concludes the paper.

## II. OFDM System Design

### A. Transmitter

This paper considers an OFDM system with one transmit and $L_r$ receive hydrophones. The proposed OFDM transmitter partitions the information symbols into packets. The packet structure is shown in Fig. 1. Each packet starts with the $T_b$-seconds-long probe signal. This signal is used for coarse synchronization at the receiver. The $T_{gb}$-seconds-long zero-padded guard interval is inserted between the probe signal and the beginning of packet. Then, each packet is partitioned into frames of length $K_f = BT_f$, where $B$ is the signal bandwidth and $T_f$ is the frame duration. To reduce the intrapacket interference, the $T_{gf}$-seconds-long zero-padded guard intervals are inserted between the frames. For ease of reference, Fig. 2 depicts the frame structure. Each frame starts with the $T_t$-seconds-long preamble (i.e., training sequence), which is used for frame synchronization and channel estimation at the receiver. Furthermore, each frame is partitioned into OFDM blocks of length $K = BT$, where $T$ denotes the block duration. The $T_g$-seconds-long cyclic prefix (CP) guard intervals are inserted between the blocks to minimize intersymbol interference (ISI). Finally, the block duration is $T' = T + T_g$, while the frame duration is $T'_f = T_f + T_{gf}$.

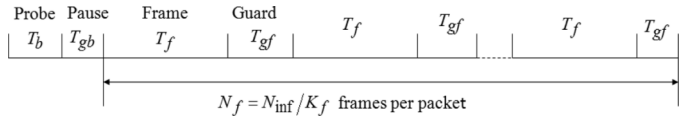


Fig. 1. Partitioning of a packet with $N_{\inf}$ symbols. Each packet begins with a probe signal of length $T_b$. After the zero-padded guard interval $T_{gb}$, the information is sent in length $T_f$ frames followed by $T_{gf}$-seconds-long zero-padded guard to reduce intrapacket interference.

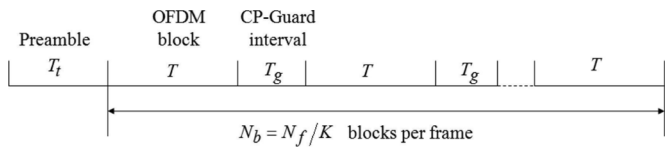


Fig. 2. Partitioning of a frame with $N_f$ symbols. The OFDM blocks are of length $K = BT$, where $B$ is the bandwidth of the signal and $T$ denotes the block duration.

Fig. 3 details the OFDM block generator structure. The information bits are coded and then interleaved. Bit-to-symbol mapping is performed using the QPSK modulation. Then, $K_p$ pilot symbols are inserted into every OFDM block. These symbols are used for the phase tracking and correction at the receiver. Furthermore, the OFDM symbols are converted from the frequency to time domain using the inverse fast Fourier transform (IFFT) and the CP guard intervals are inserted between the blocks to reduce ISI. Finally, the packets are converted from the baseband to passband and transmitted over $L_t$ transducers.

### B. Receiver

The signal at each receiver hydrophone is a superposition of the transmitted signal affected by UWA channel (which causes the amplitude fading, the multipath delay and spreading, as well as the phase distortion) and the complex additive noise. Synchronization is performed by correlating the received samples with the known $T_b$-seconds-long probing signal. After the synchronization, the received signal is converted from the passband to baseband and partitioned into frames, based on the transmission structure shown in Fig. 1.

Fig. 3 depicts frame-by-frame processing. We focus on frame-by-frame demodulation without exploiting any channel dependence across the frames. The CP is removed and then the

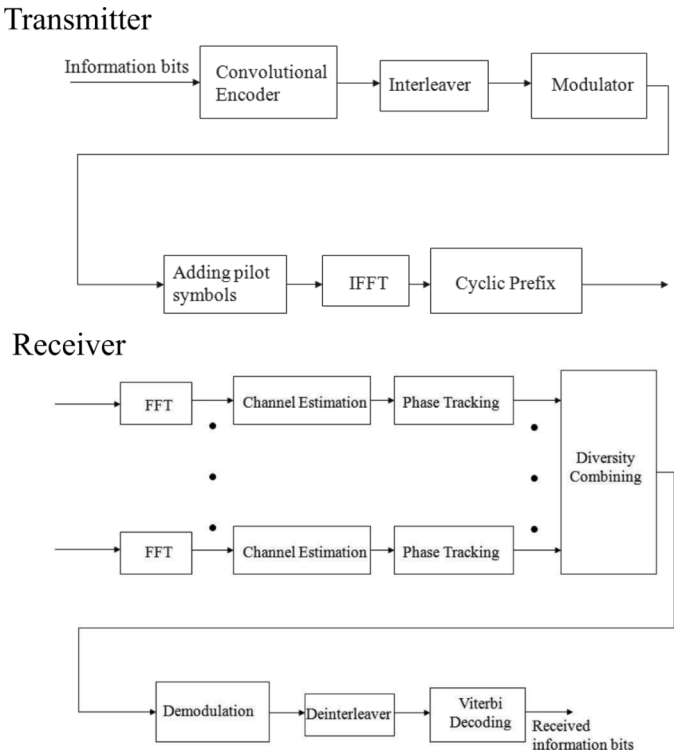


Fig. 3. Frame-by-frame OFDM transmitter and receiver. Channel estimation is done independently on each channel.

fast Fourier transform (FFT) is applied. The rest of the operations shown in Fig. 3 are described in Sections II-B1–II-B3. In particular, the channel estimation, residual phase tracking, diversity combining, demodulation, and decoding algorithms used in the proposed OFDM system are detailed.

*1) Preamble-Based Channel Estimation:* The channel estimation is performed using the $T_t$-seconds-long preamble and the least square (LS) estimation. As with prior work [4], the channel response vector is estimated on the $q$th receive hydrophone using the LS formulation shown in (1). The band-limited additive noise is denoted as $\overrightarrow{W}^{(q)}$. The transmitted preamble symbols can be combined into an $N_t \times N_t$ matrix $\mathbf{X}$. $\mathbf{F}_L$ is a matrix consisting of the first $L$ columns of the $N_t \times N_t$ unitary matrix that represents a kernel of Fourier coefficients. The time-domain channel impulse response is denoted as $\overrightarrow{h}^{(q)}$

$$\begin{bmatrix} z_0(q) \\ \vdots \\ z_{N_t-1}(q) \end{bmatrix} = \begin{bmatrix} W_0(q) \\ \vdots \\ W_{N_t-1}(q) \end{bmatrix} + \begin{bmatrix} X_0 & & \\ & \ddots & \\ & & X_{N_t-1} \end{bmatrix} \times \begin{bmatrix} e^{-j(2\pi/N_t)(0)(0)} & \cdots & e^{-j(2\pi/N_t)(0)(N_t-1)} \\ \vdots & \ddots & \vdots \\ e^{-j(2\pi/N_t)(N_t-1)(0)} & \cdots & e^{-j(2\pi/N_t)(N_t-1)(N_t-1)} \end{bmatrix} \times \begin{bmatrix} h_0(q) \\ \vdots \\ h_{N_t-1}(q) \end{bmatrix} \quad (1)$$

Note that the frequency-domain transfer function $\overrightarrow{H}^{(q)}$ can be described by

$$\overrightarrow{H}^{(q)} = \mathbf{F}_L \overrightarrow{h}^{(q)}. \quad (2)$$

Since the preamble symbols are phase-shift keying (PSK) signals with unit amplitude and the pilots are equally spaced, the LS solution of (1) simplifies to

$$\overrightarrow{\hat{h}}^{(q)} = \mathbf{F}_{\mathbf{L}}^{\mathbf{H}} X^{\mathbf{H}} \overrightarrow{z}^{(q)}. \quad (3)$$

This estimate of the time-domain channel impulse response does not involve matrix inversion.

*2) Residual Phase Tracking Algorithm:* The residual phase error occurs due to the residual carrier frequency offset and the sampling frequency offset. These offsets produce equal phase rotation in every subcarrier. Initially, the effect of the residual phase error on the BERs is small, but as the number of demodulated symbols increases, the amount of the rotation increases with every new symbol. Therefore, there is a need to track the carrier phase and ensure that the demodulated symbols never cross the decision boundaries. This is accomplished by data-aided tracking of the carrier phase, using $K_p$ predefined pilot subcarriers among the transmitted data.

After the FFT operation, the $i$th OFDM received symbol of the $n$th pilot subcarrier at the $q$th receive hydrophone, i.e., $R_{n,i}^{(q)}$, can be written as the product of the transfer function $H_{n,i}^{(q)}$ and the known pilot symbol $P_{n,i}$ rotated by the residual phase error, $\Delta\phi_i$, i.e.,

$$R_{n,i}^{(q)} = H_{n,i}^{(q)} P_{n,i} e^{j\Delta\phi_i^{(q)}}. \quad (4)$$

Using the estimated transfer function $\hat{H}_{n,i}^{(q)}$, the phase estimate is given by

$$\phi_i^{(q)} = \sphericalangle \left[ \sum_{n=1}^{K_p} R_{n,i}^{(q)} \left( \hat{H}_{n,i}^{(q)} P_{n,i} \right)^* \right] \quad (5)$$

where $\sphericalangle(\cdot)$ denotes the phase of a complex number.

*3) Diversity Combining, Demodulation, and Decoding:* The maximal ratio diversity combiner applied to each OFDM symbol can be implemented as follows [9]:

$$\overrightarrow{V} = \sum_{q=1}^{L_r} \overrightarrow{\hat{X}}^{(q)} \quad (6)$$

where after diversity combining, the symbols are demodulated, de-interleaved, and decoded using the Viterbi algorithm.

*4) Signal Design:* In both experiments, we coded the information bits using the half-rate convolutional code with generator polynomial (91, 121). Modulation is performed using the QPSK constellation, i.e., the constellation size was $M = 4$ and one information symbol carried $\log_2 M = 2$ b.

Each packet started with the $T_b = 0.3$ s long linear frequency modulated (LFM) probe signal, followed by the $T_{gb} = 0.3$ s long zero-padded guard interval. The $N_s = 19\,200$ input symbols are partitioned into $N_f = 40$ frames. The frame had $K_f = 800$ subcarriers, followed by the $T_{gf} = 0.1$ s long zero-padded

TABLE I
INPUT DATA STRUCTURE FOR THE ACOMMS09 AND SEDEX09 EXPERIMENTS

| | |
|---|---|
| Number of frame subcarriers $K_f$ | 800 |
| Number of data subcarriers in a frame $L_f K_d$ | 384 |
| Number of pilot subcarriers in a frame $L_f K_p$ | 32 |
| Number of cyclic prefix es in a frame | 128 |
| Number of preamble subcarriers $T_t B$ | 160 |
| OFDM symbol duration $T$ | 16 ms |
| Subcarrier spacing $\Delta f$ | 5 Hz |
| Frame duration $T_f$ | 0.2 s |
| Zero-padded frame guard interval $T_{gf}$ | 0.1 s |
| Bandwidth $B$ | 4 kHz |
| Number of input symbols | 19,200 |
| Number of frames in a packet | 40 |

frame guard interval. Each frame started with the $T_t = 40$ ms long preamble, followed by $L_f = 8$ OFDM blocks. The OFDM symbol duration was $T = 16$ ms and the CP guard interval was $T_g = 4$ ms. The OFDM block length was $K = 64$, where $K_d = 48$ subcarriers were used for information data and $K_p = 4$ subcarriers were used for pilot symbols. The indexes of pilot symbols were $\{12, 26, 40, 54\}$. Finally, the OFDM block duration was $T' = T + T_g = 20$ ms, while the frame duration was $T'_f = T_f + T_{gf} = 0.3$ s. For ease of reference, these parameters are summarized in Table I.

Accounting for the various transmission overhead due to coding, CP, pilot subcarriers, preamble, and zero-padded guard interval, the achieved data rate can be calculated as

$$R = r_c \log_2 M \frac{L_f K_d}{T_f + T_{gf}} \text{ [b/s]}. \tag{7}$$

Furthermore, the bandwidth utilization factor of the system can be obtained as

$$\alpha = \frac{R}{B} = r_c \log_2 M \frac{T_f}{T_f + T_{gf}} \frac{L_f K_d}{K_f} \text{ [b/s/Hz]}. \tag{8}$$

The data rates for uncoded and coded SISO QPSK OFDM signals are $R = 2560$ b/s and $R_{\text{coded}} = 1280$ b/s, respectively. For half coding rate, the bandwidth utilization factor is $\alpha = 0.32$ b/s/Hz. Note that the data rate and the bandwidth utilization factor can be improved by choosing shorter zero-padded frame guard interval. Conservatively, the frame guard interval was chosen to be $T_{gf} = 0.1$ s, although it can be $T_{gf} = 0.05$ s or less, without the performance degradation. Here, the main goal was to provide reliable communications between buried nodes.

## III. DESCRIPTION OF ACOMMS09 AND SEDEX09 EXPERIMENTS

This section describes several measurement settings used during the ACOMMS09 and SedEx09 experiments.

### A. ACOMMS09 Experiment

The experimental data were collected near the New Jersey shore in May 2009. The water depth was about 80 m and the sediment was a silty clay. The details about the experimental site can be found in [10].

To test the proposed OFDM system, we have first performed an experiment using three stationary vertical arrays placed near the water column. The stationary vertical source receiver array (ASRA) was about 45.57 m below the surface float and it had eight transducers with the aperture 0.8 m. We have only used the first transducer for transmission. On the receiver side, we have used two stationary receive arrays. The first receive array (ACDS2) was 19.66 m below the surface float, while the second receive array (ACDS3) was 41.96 m below the surface float. Both receive arrays had eight hydrophones with the aperture 2.06 m, where we have only used the first four hydrophones for reception. The ACDS2 receiver was on the right-hand side of the transmitter, 2000 m away, while the ACDS3 receiver was on the left-hand side of the transmitter, 1500 m away. The center frequency was $f_c = 17$ kHz, and the signal bandwidth was $B = 4$ kHz. Finally, the sampling rate was $f_s = 93.75$ kHz.

To test the underwater communications between the buried and near-bottom hydrophones, we deployed a stationary three-element vertical array anchored with three hydrophones mounted on a sediment penetrating frame. This array was collocated with ACDS2 array. The three buried hydrophones were attached below a heavy metal triangular grid that was dropped on the ocean floor. The hydrophones were driven (about 15 cm) into the soft sediment (i.e., mud). In our signal processing, we have used only the first one because it was the most buried hydrophone. The first hydrophone in the vertical array was attached to the metal grid about 60 cm above the ocean floor. The second and third hydrophones were 120 and 217 cm above the ocean floor, respectively. All signals were transmitted from the first hydrophone in ASRA array. The center frequency was $f_c = 17$ kHz, and the signal bandwidth was $B = 4$ kHz. Finally, the sampling rate was $f_s = 93.75$ kHz.

### B. SedEx09 Experiment

The second experimental data set was collected near Panama City, FL, in August 2009. The range-independent environment was about 10 m deep with a hard sandy bottom. The fixed transmitter consisted of four transducers. The first was buried about 10 cm deep, while the rest were, respectively, placed at 0.5, 1, and 2 m from the bottom. The receive system consisted of four hydrophones with the first buried 10 cm below the bottom and the rest, respectively, placed 0.5, 1, and 2 m from the bottom. Divers deployed both systems and moved the receive system in range from 200 to 600 m. The center frequency was $f_c = 17$ kHz, and the signal bandwidth was $B = 4$ kHz. Finally, the sampling rate was $f_s = 100$ kHz. Unlike the previous geometry where a midwater column transducer was communicating with receive systems located at shallow and deep positions in the waveguide, this geometry is reciprocal in depth between transmit and receive systems.

## IV. EXPERIMENTAL RESULTS

This section presents measured channel impulse response (CIR), SNR, and BER for experimental settings described in Section III and evaluates the feasibility of underwater communications between buried sensor nodes.

TABLE II
SNR AND BER RESULTS FOR UNCODED AND CODED SISO QPSK SIGNALS RECEIVED BY ACDS2 AND ACDS3 IN NEW JERSEY

| Packets received at ACDS3 | QPSK SNR [dB] | Uncoded BER for SISO QPSK | Coded BER for SISO QPSK | Packets received at ACDS2 | QPSK SNR [dB] | Uncoded BER for SISO QPSK | Coded BER for SISO QPSK |
|---|---|---|---|---|---|---|---|
| … | … | … | … | … | … | … | … |
| 21 | 12.89 | 0.061 | 0 | 10 | 11.7 | 0.057 | 0 |
| 22 | 12.6 | 0.074 | 0 | 11 | 13.58 | 0.06 | 0.0025 |
| 23 | 12.34 | 0.056 | 0 | 12 | 11.82 | 0.078 | 0.003 |
| 24 | 15.1 | 0.034 | 0.0008 | 13 | 8.91 | 0.056 | 0.01 |
| 25 | 15.11 | 0.024 | 0 | 14 | 7.81 | 0.084 | 0.00059 |
| 26 | 14.78 | 0.036 | 0 | 15 | 11.28 | 0.03 | 0 |
| 27 | 11 | 0.06 | 0.0018 | 16 | 7.22 | 0.079 | 0 |
| 28 | 14.1 | 0.075 | 0.0055 | 17 | 10.92 | 0.07 | 0.032 |
| 29 | 18.45 | 0.021 | 0 | 18 | 11.4 | 0.06 | 0 |
| 30 | 20.5 | 0.022 | 0.00029 | 19 | 12.53 | 0.051 | 0 |
| … | … | … | … | … | … | … | … |
| Average over 35 packets | 13.555 | $5.64\cdot10^{-2}$ | $3.35\cdot10^{-3}$ | Average over 35 packets | 10.47 | $7.2\cdot10^{-2}$ | $6.12\cdot10^{-3}$ |

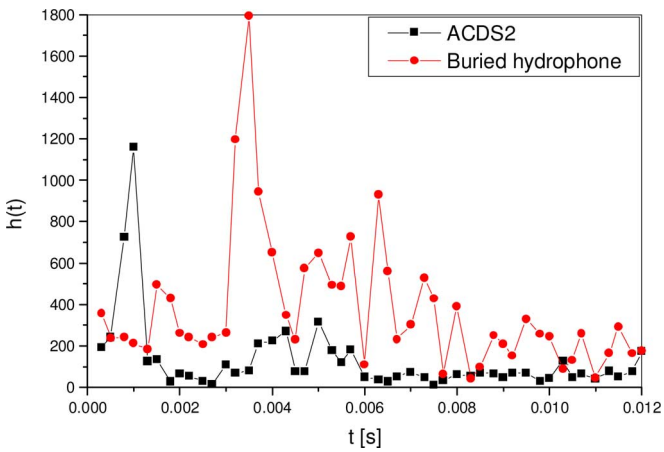


Fig. 4. The typical channel impulse responses measured at the first element of ACDS2 array and at the buried hydrophone. In New Jersey, the buried hydrophone measured a large number of propagation paths from the source at 45-m depth compared to a receiver at about 20-m depth.

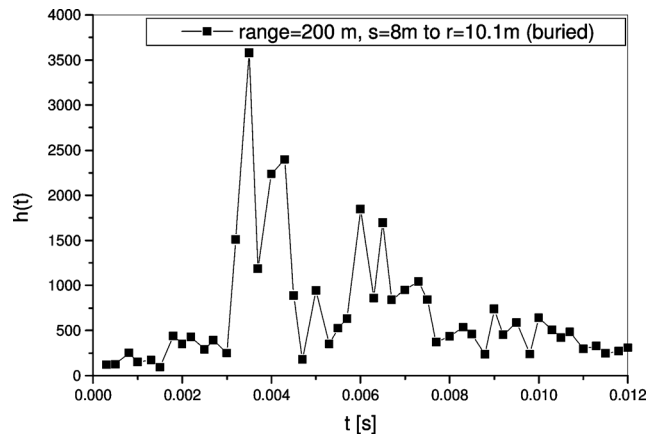


Fig. 5. The typical CIR estimated between the buried hydrophone and the hydrophone placed 2 m from the ocean floor in Panama City Beach, FL.

### A. The Results From the ACOMMS09 Experiment

To test the proposed OFDM system, we have first performed an experiment using three arrays (ASRA, ACDS2, and ACDS3) placed near the water column. The SNR and BER results for SISO uncoded and coded QPSK signals received by ACDS2 and ACDS3 are summarized in Table II, which exemplifies intrapacket variability. The results show that the ACDS3 receiver has slightly higher SNR than ACDS2 receiver. This is an expected result because the ACDS3 receiver is closer to the transmitter ($R = 1500$ m) than the ACDS2 receiver ($R = 2000$ m). The uncoded BER for SISO QPSK signals is about $10^{-2}$, while the coded BER for SISO QPSK signals is about $10^{-3}$. The similar BERs are observed at both receivers. Compared to the ACDS2 receiver, the ACDS3 receiver has slightly smaller BER due to higher SNR. Table II also shows that it is possible to receive SISO QPSK packets without errors. These results have encouraged us to use the proposed OFDM system to test underwater communications between buried hydrophones.

The typical CIRs estimated at the first element of ACDS2 array and at the buried hydrophone are presented in Fig. 4. Recall that the buried hydrophones are collocated with ACDS2 and that the source is at about midwater column depth. The results show that the CIR estimated at the buried hydrophone has much larger number of propagation paths compared to CIR estimated at ACDS2. Furthermore, the results show that the first arriving ray is the most dominant component of the CIR estimated at ACDS2, while the second and third rays are the most dominant components of the CIR estimated at the buried hydrophone. All these results illustrate the differences between underwater propagation near the water column and near the ocean floor and show the challenges needed to overcome when placing sensor network nodes near the ocean floor.

The measured SNR collected at the buried hydrophone and the hydrophones placed 60, 120, and 217 cm above the ocean floor, respectively, are summarized in Fig. 6(a). The results show that the buried hydrophone and the hydrophone

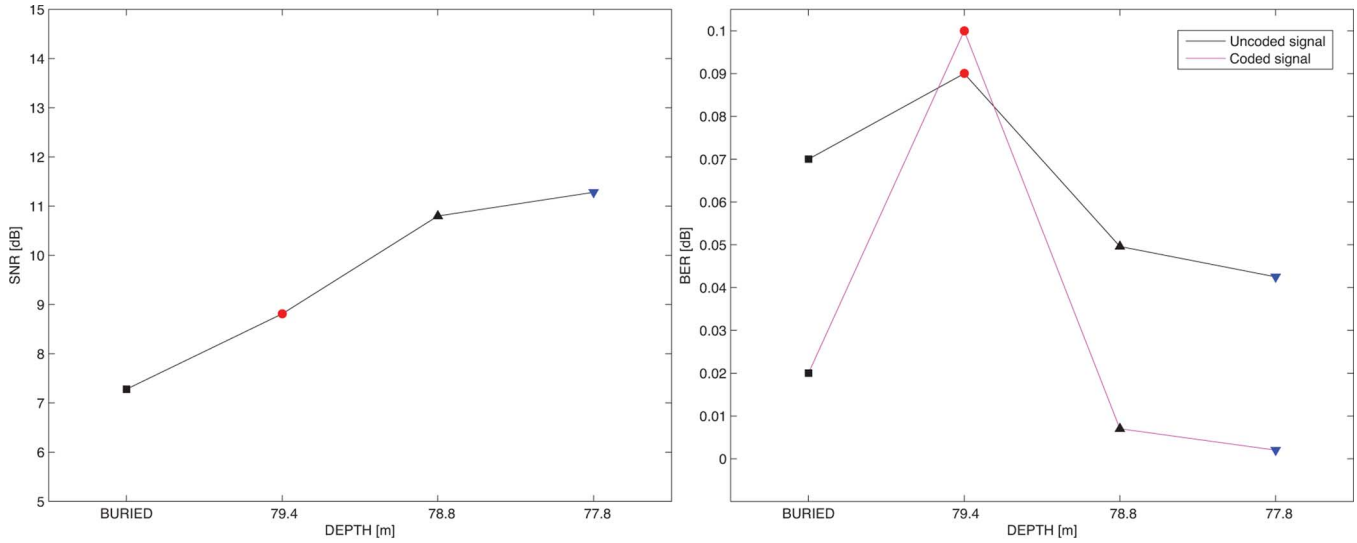


Fig. 6. SNR and BER as a function of depth between a transmitter at a depth of 46 m to receivers 1500 m away in approximate ocean depth of 80 m.

placed 60 cm above the ocean floor have an average SNR that is less than 10 dB. As expected, this low SNR is not sufficient to achieve reliable communications because it leads to unacceptable BERs. On the other hand, the hydrophones placed 120 and 217 cm above the ocean floor have an average SNR that is higher than 10 dB, which is sufficient to achieve acceptable BERs for all packets (i.e., $10^{-2}$). Intriguingly, the SNR difference between the buried hydrophone and the lowest waterborne hydrophone (60 cm above the ocean floor) was about 1.5 dB on average.

Using only the packets with SNR higher than 8 dB, we have calculated BER using the proposed OFDM system. The BER results obtained for the buried hydrophone and the hydrophones placed 60, 120, and 217 cm above the ocean floor, respectively, are summarized in Fig. 6(b). The averaged uncoded and coded BERs for SISO QPSK signals collected at the buried hydrophone are $7 \times 10^{-2}$ and $2 \times 10^{-2}$, respectively. The similar results are obtained for the hydrophone placed 60 cm above the ocean floor. On the other hand, the averaged uncoded and coded BERs for SISO QPSK signals collected at the hydrophones placed 120 and 217 cm above the ocean floor are about $10^{-2}$ and $10^{-3}$, respectively.

The results presented in Fig. 5 imply that if sufficient SNR is available, the uncoded and coded BERs for SISO QPSK signals are about $10^{-2}$ and $10^{-3}$, respectively, regardless of how close to the ocean floor sensor nodes are placed. Note that the similar BERs are obtained with ACDS2 hydrophone array which was placed in the upper water column. These results suggest that the main obstacle in achieving reliable communications with sensor nodes buried in the soft sediment lies in providing sufficient SNR to the receiving system. Furthermore, the communication system was robust to changes in the CIR and variability between buried and near-bottom configurations.

### *B. The Results From the SedEx09 Experiment*

The typical CIR estimated between the buried source and the hydrophone placed 2 m from the ocean floor is presented in Fig. 6. Similar to the CIR estimated at the hydrophones buried in the soft sediment, the CIR estimated at the hydrophones buried in the hard sediment has a large number of propagation paths, where the later rays are more dominant than the first arriving ray. Note that no acoustic energy passes directly through the sediment due to strong attenuation.

Fig. 7 plots SNR and BER measured during the SedEx09 experiment as a function of the distance between the transmitter and the receiver. Fig. 7(a) and (b) plots SNR and BER, which were obtained by the following scenario: the signal was transmitted from the transducer placed 2 m from the ocean floor and received at the buried hydrophone and the hydrophones placed 0.5, 1, and 2 m from the ocean floor, respectively. The results in Fig. 7(a) show that the link between hydrophones placed 2 m from the ocean floor has the strongest signal, while the link between the buried hydrophone and the hydrophone placed 2 m from the ocean floor has the weakest signal. The results also show that we had sufficient SNR to achieve reliable communications for all ranges and depths. The results in Fig. 7(b) show that for this experimental setup, coded BER for SISO QPSK signals was zero regardless of the receiving hydrophone depth. On the other hand, the uncoded BERs for SISO QPSK signals collected at the buried hydrophone and the hydrophone placed 0.5 m above the ocean floor are about $10^{-2}$, while the uncoded BERs for SISO QPSK signals collected at the hydrophones placed 1 and 2 m above the ocean floor are about $10^{-3}$. Note that the BER increases with the distance between the transmitter and the receiver, which corresponds to the decrease in the available SNR. Fig. 7 implies a change in the channel characteristics between sensors above and below approximately 1 m.

Fig. 7(c) and (d) shows SNR and BER obtained when the signal was transmitted from the buried source and received at the buried hydrophone and the hydrophones placed 0.5, 1, and 2 m from the ocean floor, respectively. The results show sufficient SNR at all four hydrophones to achieve reliable com-

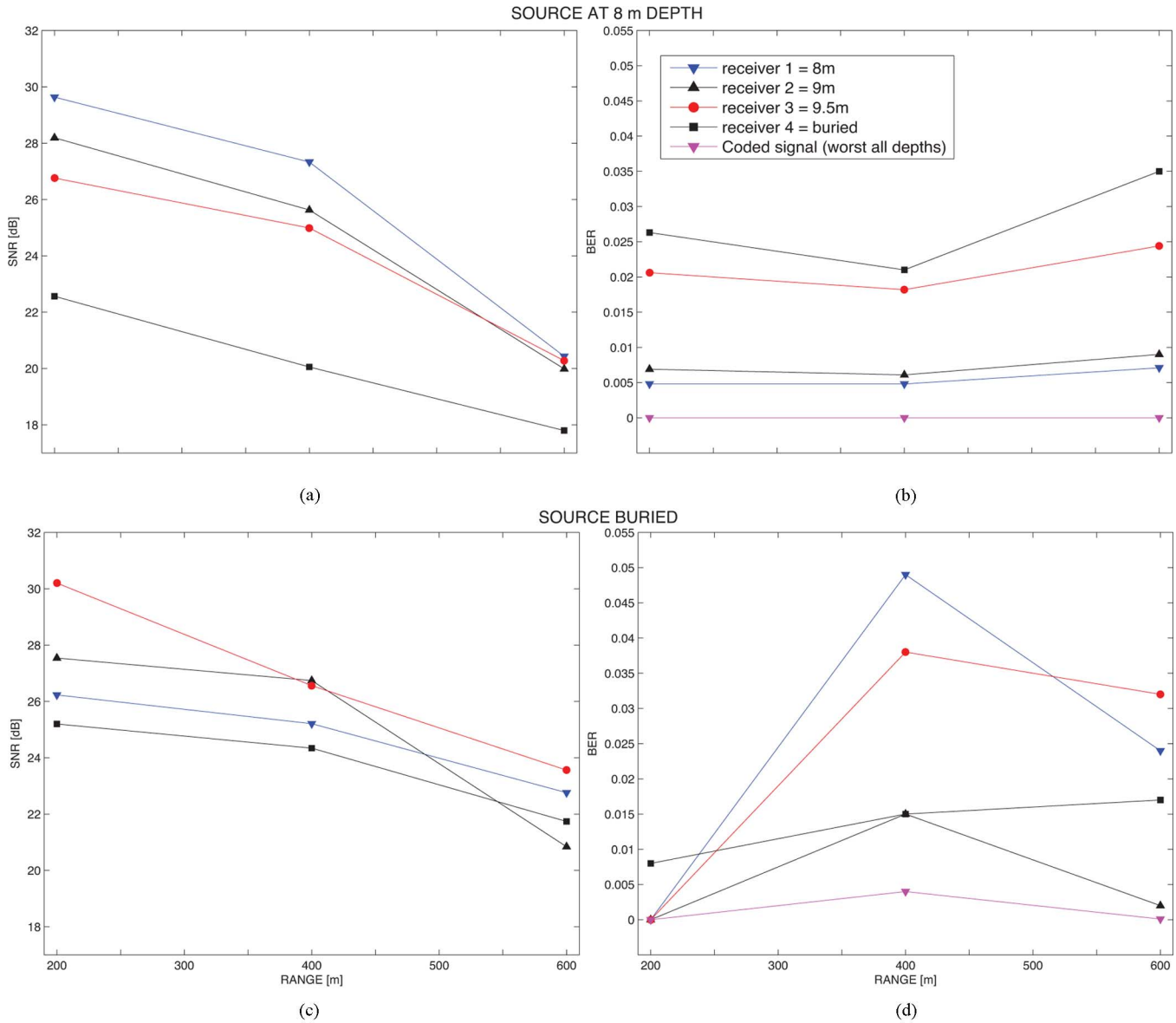


Fig. 7. (a) and (b) SNR and BER as a function of distance between a transmitter at 8 m and multiple receivers in Panama City Beach, FL. In a geometry where bottom-mounted systems communicate with each other, the mast height had little effect on SNR as shown in (a). The difference between buried and waterborne sensors was only 2 dB at 600 m. (b) BER as a function of range and depth. Although there was enough SNR to achieve reliable communications at all depths, SNR does not tell the whole story; moving the mast away from the bottom improves the reception. The performance of a 1-m mast was comparable to that of a 2-m mast. (c) and (d) SNR and BER for a buried source. Due to the different propagation, the received SNR is counterintuitively best for the 0.5-m mast and the buried receiver has improved signal strength. The uncoded BER is superior for the 1-m mast. However, buried-to-buried communication has consistent BER of about $10^{-2}$.

munications. The averaged uncoded and coded BERs for SISO QPSK signals collected at the buried hydrophone are $10^{-2}$ and $10^{-4}$, respectively. On the other hand, the averaged uncoded and coded BERs for SISO QPSK signals collected at the hydrophones placed 0.5, 1, and 2 m above the ocean floor are about $10^{-2}$ and 0, respectively. Quite significantly, these results show that the proposed OFDM scheme can handle a large number of strong propagation paths if sufficient SNR is available (i.e., $>$10 dB). Furthermore, it is possible for completely buried systems to communicate with one another at short ranges or high SNR.

The performance of the proposed SISO OFDM system can be improved by superimposing the signals received by all of the elements of the receive hydrophone array. Compared with the results of Table II, the ACDS2 SNR, BER, and coded BER improved to 15.57, 0.0074, and 0, respectively, and the ACDS3 SNR, BER, and coded BER improved to 15.12, 0.005, and 0, respectively. By combining the buried and unburied array measurements in New Jersey, the SNR, BER, and coded BER improved to 12.58, 0.003, and 0, respectively, as compared with Fig. 5. Last, the signals, measured on the four elements of the hydrophone array in Panama City, combined yield an SNR, BER, and coded BER improvement of 24.65, 0.0045, and 0, respectively, at 600 m from the buried source, as compared with Fig. 7. The results show that the average input SNR of the combined arrays in all experimental setups is higher than 10 dB,

which is sufficient to receive signal with a small number of errors. Furthermore, the results show that all four setups have the uncoded BER about $10^{-3}$, while the coded signals are received without errors.

## V. Conclusion

This paper presented the feasibility study of underwater communications between buried sensor network nodes. To investigate this problem, two experiments were conducted: one where sensor network nodes are buried in the soft sediment, and the second one where the sensor network nodes were buried in the hard sediment. The new, low-complexity OFDM receiver was designed to combat a large number of strong propagation paths that are distorting signal near the ocean floor. The proposed receiver performs frame-by-frame channel estimation, residual phase tracking, diversity combining, and data demodulation.

The presented results show that communication among buried distributed sensors is possible. They also show that using the proposed OFDM receiver, error-free communications can be achieved among buried distributed sensors. Furthermore, the results indicate that the performance of sensor nodes at about 1 and 2 m above the ocean floor have similar both SNR and BER. Finally, the results show that SNR is degraded by about 2 dB by being buried just below the sediment. All presented results indicate that to achieve reliable underwater communications between buried distributed sensors, we need to design a system that has high SNR, can successfully handle the large number of propagation paths, and uses multiple hydrophones as receiving elements.

## References

[1] W. Lynn, "3D, 4D, and beyond," *J. Petroleum Eng.*, pp. 35–35, Jan. 1998.

[2] J. Proakis, J. Rice, and M. Stojanovic, "Shallow water acoustic networks," *IEEE Commun. Mag.*, vol. 39, no. 11, pp. 114–119, Nov. 2001.

[3] M. Stojanovic, "Low complexity OFDM detector for underwater channels," in *Proc. MTS/IEEE OCEANS Conf.*, Boston, MA, Sep. 18–21, 2006, DOI: 10.1109/OCEANS.2006.307057.

[4] B. Li, S. Zhou, M. Stojanovic, L. Freitag, and P. Willett, "Multicarrier communication over underwater acoustic channels with nonuniform Doppler shifts," *IEEE J. Ocean. Eng.*, vol. 33, no. 2, pp. 198–209, Apr. 2008.

[5] B. Li, S. Zhou, M. Stojanovic, L. Freitag, J. Huang, and P. Willett, "MIMO-OFDM over an underwater acoustic channel," in *Proc. MTS/IEEE OCEANS Conf.*, Vancouver, BC, Canada, Oct. 2007, DOI: 10.1109/OCEANS.2007.4449296.

[6] B. Li, S. Zhou, J. Huang, and P. Willett, "Scalable OFDM design for underwater acoustic communications," in *Proc. Int. Conf. Acoust. Speech Signal Process.*, Apr. 2008, pp. 5304–5307.

[7] B. Li, J. Huang, S. Zhou, K. Ball, M. Stojanovic, L. Freitag, and P. Willett, "MIMO-OFDM for high-rate underwater communications," *IEEE J. Ocean. Eng.*, vol. 34, no. 4, pp. 634–644, Oct. 2009.

[8] P. J. Gendron, "Orthogonal frequency division multiplexing with on-off-keying: Noncoherent performance bounds, receiver design, and experimental results," *U.S. Navy J. Underwater Acoust.*, vol. 56, no. 2, pp. 267–300, Apr. 2006.

[9] G. L. Stüber, *Principles of Mobile Communication*. Norwell, MA: Kluwer, 2001, ch. 6, pp. 280–284.

[10] J. R. Apel, M. Badiey, C.-S. Chiu, S. Finette, R. Headrick, J. Kemp, J. F. Lynch, A. Newhall, M. H. Orr, B. H. Pasewark, D. Tielbuerger, A. Turgut, K. Von Der Heydt, and S. Wolf, "An overview of the 1995 SWARM Shallow Water Internal Wave Acoustic Scattering Experiment," *IEEE J. Ocean. Eng.*, vol. 22, no. 3, pp. 465–500, Jul. 1997.

**Alenka G. Zajić** (S'99–M'08) received the B.S. and M.S. degrees in electrical engineering from the School of Electrical Engineering, University of Belgrade, Belgrade, Serbia, 2001 and 2003, respectively, and the Ph.D. degree from the School of Electrical and Computer Engineering, Georgia Institute of Technology, Atlanta, in 2008.

She is an Assistant Professor in the School of Electrical and Computer Engineering, Georgia Institute of Technology, Atlanta. Before that, she was visiting faculty in the School of Computer Science at Georgia Tech, a Postdoctoral Fellow in the Naval Research Laboratory, and a Design Engineer at Skyworks Solutions Inc. Her research interests span areas of electromagnetics, wireless communications, signal processing, and computer engineering.

Dr. Zajić received the Best Paper Award at the 2008 International Conference in Telecommunications, the Best Student Paper Award at the 2007 Wireless Communications and Networking Conference, and was also the recipient of the Dan Noble Fellowship in 2004, awarded by Motorola Inc. and the IEEE Vehicular Technology Society for quality impact in the area of vehicular technology.

**Geoffrey F. Edelmann** received the B.S. degree in physics from the University of California San Diego, La Jolla, in 1997 and the Ph.D. degree in oceanography from the Scripps Institution of Oceanography, San Diego, CA, in 2003.

Currently, he is a Research Physicist at the U.S. Naval Research Laboratory, Washington, DC. His current research interests include data telemetry, networking, propagation modeling, compressive sensing, time reversal, internal waves, beamforming, matched field processing, and other acoustic signal processing both in the air and sea.